Journal of Colloid and Interface Science 664 (2024) 972–979

Contents lists available at ScienceDirect

Journal of Colloid And Interface Science

journal homepage: www.elsevier.com/locate/jcis

Regular Article

Determination of the optimal pH for doxorubicin encapsulation in polymeric micelles

Lucrezia Desiderio [a,1], Natalie Solfried Gjerde [a,1], Elisamaria Tasca [a], Luciano Galantini [a], Irantzu Llarena [b], Paolo Di Gianvincenzo [b], Sunisa Thongsom [b], Sergio E. Moya [b,*], Mauro Giustini [a,c,*]

[a] Chemistry Department, University of Rome "La Sapienza", P.le Aldo Moro 5, 00185 Rome, Italy
[b] CIC biomaGUNE, Paseo Miramon 182, 20011 San Sebastián, Spain
[c] CSGI c/o Chemistry Department, University of Bari, Via Orabona 4, 70126 Bari, Italy

GRAPHICAL ABSTRACT

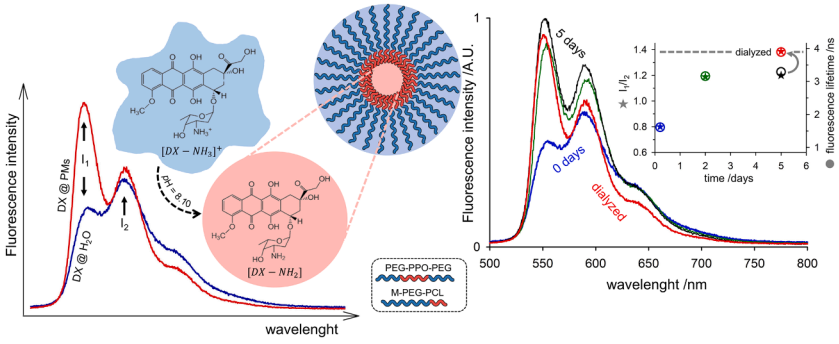

ABSTRACT

Hypothesis: The anticancer drug doxorubicin hydrochloride (DX) shows a high solubility in aqueous media thanks to the positive charge in the ammonium group. This feature, however, affects the drug encapsulation in the hydrophobic domains of polymeric micelles (PMs) used for the targeted delivery of the drug. At basic pH, DX deprotonates but also acquires a negative charge in the phenolic groups of the anthracycline structure. Both the efficiency and the rate of encapsulation will be increased by choosing an appropriate pH such that the drug molecule is in neutral form.

Experiments: An optimal pH for the encapsulation of the DX in PMs based on commercial poloxamers and on the diblock copolymer methoxy-poly(ethylene glycol)$_{17}$-*b*-poly(ε-caprolactone)$_9$ was determined by fluorescence spectroscopy, following the time evolution of both the intensity ratio of the first and the second emission bands of DX and its fluorescence lifetime, both sensitive to the environment polarity. Intracellular delivery of PMs encapsulated drug was followed by Confocal Scanning Laser Microscopy (CSLM). Cell viability was assessed with the sulforhodamine B (SRB) assay.

Findings: By adjusting pH to 8.1 a high yield of incorporation of DX in the PMs was achieved coupled to an appreciable increase (one order of magnitude) in the drug encapsulation rate. *In-vitro* tests in selected cancer cell lines showed the slow release of the drug and a delay in the cytotoxic response in comparison to free DX as detected by CSLM and SRB assay. The proposed methodology paves the way for a greener, faster and more efficient encapsulation of DX in PMs.

* Corresponding authors.
E-mail addresses: smoya@cicbiomagune.es (S.E. Moya), mauro.giustini@uniroma1.it (M. Giustini).
[1] These authors contribute equally to the work.

https://doi.org/10.1016/j.jcis.2024.03.101
Received 10 January 2024; Received in revised form 27 February 2024; Accepted 14 March 2024
Available online 15 March 2024

1. Introduction

Doxorubicin hydrochloride (DX – Chart 1) is a well-known chemotherapeutic drug belonging to the anthracycline family. DX has a relatively high water solubility and easily enters in the cells, trespassing cell membrane and translocating into the nucleus [1]. There, the drug intercalates between adjacent base pairs of DNA, interfering with both cell translation and replication, thus inducing cell death [2–4]. Intravenous administration of free DX leads to unspecific toxicological endpoints in any accessible tissue not only into the target tumour. In addition, DX is known to be cardiotoxic. The design of carriers that prevent or decrease DX delivery outside tumour tissue and selectively favour a controlled release of the drug intratumorally, is therefore of pivotal importance for its therapeutic applications. Indeed, some liposomial based drug carriers have reached the marked since several years. Myocet® (made of non-pegylated lipids), Doxyl®/Caelyx® (pegylated-liposomes) are currently available for the managements of several malignancies [5,6]. Though showing an ameliorate pharmacokinetics compared to the free drug [7], they still suffer from some limitations in their use, mostly because of their dimensions and composition of the bilayer [8]. Polymeric carriers could bring advantages on DX delivery due to their high stability and low toxicity [9].

Recently our group proposed a polymeric mixed micellar system based on pluronic polymers for the encapsulation of DX showing an extremely promising potential as delivery system [10,11]. DX was encapsulated in the hydrophobic core of the micelles by a progressive deprotonation of its ammonium group triggered by the presence of the bile salt sodium cholate (NaC).

Although attractive due to the high incorporation yield in the micelles and slow release of the drug to target cells, which resulted in a more progressive uptake in the nuclei compared to the free drug, the approach followed for DX encapsulation had an extremely slow drug internalisation kinetics. Up to two months were required to reach maximum drug uptake in the micellar phase [10,11]. Being interested in preparing a polymeric micellar system for drug delivery applications, in the previous works we limited the number of the chemicals to the minimum, just poloxamer F127, NaC and DX without any buffering agent since the pH of the resulting solution remained always not far from neutrality (around 7.7) throughout the encapsulation procedure [10,11].

A plausible reason for the slow kinetics of incorporation of DX into the apolar F127 poloxamer micellar core could be found in the cationic nature of DX preventing its solubilisation in apolar media. The treatment of DX with mild bases, such as trimethylamine or triethylamine, to convert it into its unprotonated form (DX-NH_2) has been indeed reported in the literature to ease the DX incorporation into the hydrophobic core of polymeric micelles [12–15].

Since the DX ammonium group is located relatively far from the anthraquinone chromophore/fluorophore moiety of the molecule, its deprotonation results only into a barely appreciable decrease in both the drug molar extinction coefficient and fluorescence quantum yield without any other significant variation in the shape of the absorption/emission spectrum. The deprotonation constant of the DX ammonium group (pK_{CN}) has been estimated by several authors, and a spread of values can be found in the literature, covering a relatively wide range, from a minimum of 6.80 to a maximum of 9.25 [16–22], mostly depending on the DX concentration and, therefore, on the degree of DX dimerization [23], as well as on the experimental approach used for its determination. Moreover, its determination often relies on fitting the absorbance data of the evolution of DX spectra with pH. One of the main characteristics of the drug in the free base form is its markedly reduced solubility in water [24] and as a consequence, when in the DX-NH_2 form, the drug is prone to dissolve in apolar environments, such as the PPO core of poloxamer micelles [25] or other polymeric micelles formed by amphipathic copolymers.

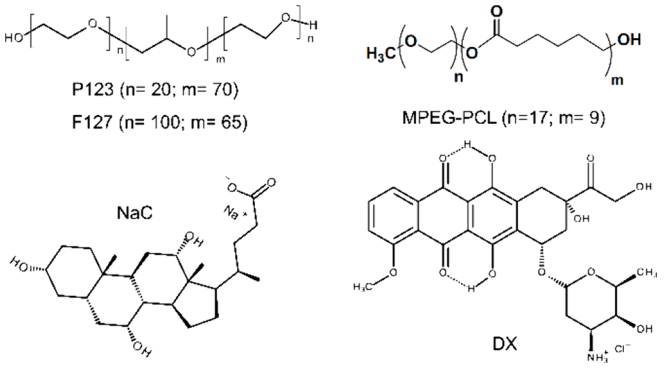

Chart 1. Chemical formulae of pluronics F127 and P123, of the MPEG-PCL copolymer (Z233), of sodium cholate (NaC) and of doxorubicin hydrochloride (DX).

Recently we investigated the electronic properties of DX combining spectroscopic data and molecular dynamics (MD) simulations that revealed that the spectral shape assumed by the drug when solubilized in the core of poloxamer/NaC mixed micelles strongly resemble that of DX-NH_2 dissolved in apolar solvents/media [26]. While basic pHs induce deprotonation of the ammonium group in DX, they can also lead to the loss of protons from the phenolic groups of the anthraquinone; a negative charge will then appear, decreasing the drug solubility in an organic phase (the whole set of doxorubicin deprotonation equilibria and the relevant drug absorption spectra at different pHs are reported in Fig. A1). Therefore, a convenient pH must be found for encapsulation of DX in the inner core of the micelles that will ensure the ammonium group to be (mostly) deprotonated while minimizing the appearance of any negative charge on the phenolic groups.

The aim of the present work is to reduce the time required for the preparation of polymeric micelles (PM) incorporating DX by determining the optimal pH for the transfer of DX from the aqueous environment to the apolar core of the PM and to propose an explanation for the slow kinetics of incorporation of DX reported in previous works of our group [10,11]. To evaluate the optimal pH for encapsulating DX in the apolar environment, the partition of DX between water and chloroform was assessed by UV and fluorescence spectroscopy at different pHs in the range from 6.5 to 8.5 while the deprotonation of the phenolic group of the anthraquinone was traced by the appearance of an UV band at 590 nm [22]. Profiting from the sensitivity of DX fluorescence to the polarity of the environment, it was possible to assess the kinetics of incorporation of the drug inside PM by the change in the intensity ratio of the first and second emission bands of DX (I_1 and I_2, respectively) and through the measurement of the drug fluorescence lifetime. Physicochemical characterization was complemented with cell proliferation studies and Confocal Scanning Microscopy (CLSM) to assess the impact of DX encapsulation on cell toxicity and on the intracellular drug release.

It has to be further added that the preparation method here proposed represents a greener alternative to those presented in the literature because it avoids the use of any organic chlorinated solvent.

2. Materials and methods

The chemical structure of the main chemicals used in this work is shown in Chart 1. Unless otherwise stated, all the chemicals were purchased from Sigma-Aldrich and of the highest purity available and used without further purification. The diblock copolymer methoxy-poly(ethylene glycol)$_{17}$-*b*-poly(ε-caprolactone)$_9$ (MPEG-PCL - Z233) was a kind gift of Prof. Bo Nyström. MPEG-PCL was prepared by ring-opening polymerization of ε-caprolactone with MPEG as the initiator and stannous octoate as the catalyst, as elsewhere described [27]). Doxorubicin hydrochloride (DX; ≥ 98 %) was a kind gift of Farmitalia-Carlo Erba Chem. Co. Ultrapure water (18.2 MΩ/cm) from Arium pro UV system (Sartorius Stedim Biotech) was used in the preparation of the solutions.

Samples were prepared by weighing the polymers, F127/P123 and Z233 (Table 1), and then adding 5.0 mL of a Tris•HCl solution (0.05 M); final pH for all the samples: 8.10 ± 0.05. In the case of pluronic-based micelles, the solutions were stored overnight under mild stirring at 4 °C, then brought to room temperature for 1 hr to be finally incubated at 45 °C. MPEG-PCL, instead, were directly heated at 45 °C after mixing at room temperature. This temperature was chosen because is higher than the critical micellization temperature (CMT) of the polymers used that, in particular for Z233, was in the interval 40–50 °C [27]. DX was then added to the samples from a concentrated water stock solution ($[DX]_{stock} = 1.7•10^{-2}$ mol/L). In all the samples, the final DX concentration ($[DX]_{anal}$) was around $1.7•10^{-4}$ mol/L. The actual DX initial concentration, $[DX]_{starting}$, in each sample was measured by UV–Vis spectroscopy, as described in the Appendix. In all the cases, samples were kept under continuous mild stirring in the dark and at 45 °C in a thermostatic bath (Julabo CF31 equipped with a Pt100 temperature probe; Julabo GmbH - Germany). At selected time points, about 120 μL of each sample were transferred in a prewarmed (45 °C) fluorescence cuvette (0.3 × 0.3 pathlength; Starna GmbH - Germany) for fluorescence (both steady state and time resolved), UV–Vis and dynamic light scattering (DLS) measurements. After the measurements, the solutions were transferred back to the tubes. During all these procedures, the utmost care was paid to avoid any variation in the temperature of the samples, that remained always fixed at 45 ± 0.5 °C.

To remove the non internalized drug, the PMs were dialyzed against a calf thymus DNA (ctDNA; 42 % in GC base pairs) solution at 45 °C under mild stirring, according to an already published procedure [10,11], that allowed to limit the dialysis time to few hours without any change of buffer, therefore limiting the drug leaking from the PMs. Briefly, Hamilton Pur-A-Lyzer™ dialysis tubes were used with a cut off of 1000 g/mol. ct-DNA was obtained from Serva in vials of 250 mg and was used as received. A stock ctDNA water solution was prepared by dissolving 22.2 mg of the polynucleotide (average molecular weight $8.58•10^6$ g/mol [28]) in 20 mL ultrapure water; the resulting solution, once diluted 1:10 directly in a 0.4 cm pathlength quartz cuvette, had an absorbance at 260 nm ($\varepsilon_{260nm} = 6600\ M^{-1}cm^{-1}$ [29]) of 1.12, from which a concentration (in phosphate groups) of $[ctDNA]_P = 4.24•10^{-4}$ M was calculated. The volume of ct-DNA solution used in the dialysis buffer ([Tris•HCl] = 0.05 M; 8.10 ± 0.05) was such to have a final molar ratio of $[ctDNA]_P/[DX]_{anal} \approx 6$. After the dialysis, fluorescence (both steady state and time resolved), UV–Vis and DLS of the samples were checked again and then the samples were freeze-dried and stored under Ar at −25 °C. The concentration of the internalized DX-NH_2 was determined by the absorbance at 541 nm ($\epsilon_{541\ nm} = 7319\ M^{-1}cm^{-1}$) [26] where a well-defined peak can be observed in the absorption spectra of dialyzed samples, according to a procedure detailed described below and in the Appendix.

DLS measurements were performed with a Zetasizer Nano ZS instrument (Malvern Instruments Ltd., Worcestershire, UK), equipped with a 5 mW HeNe laser (λ = 632.8 nm) and a digital logarithmic correlator. The normalized intensity autocorrelation functions were measured at a fixed angle of 173°. The temperature was fixed to 45 °C by the Peltier-thermostatted sample holder of the instrument (accuracy: ± 0.1 °C).

Steady state fluorescence measurements were performed with a Fluoromax 2 (Horiba-Jobin Yvon) spectrofluorometer equipped with a Peltier-thermostatted sample holder (Quantum Northwest, Liberty Lake, WA, USA) controlled by the TC1 unit via the *T*-App software from the same manufacturer. Sample temperature was measured through the QNW-2 thermistor probe dipped in the cuvette and directly connected to the TC-1 unit (accuracy: ± 0.01 °C). Excitation wavelength, slits width and filters (if used) information will be provided in due time. UV–Vis spectra were measured with a Varian Cary 5E instrument. Fluorescence lifetime measurements were performed with a home-build apparatus described in a previous work.[10].

Table 1
Weighted mass and molar mass of the polymers used for samples preparation.

Sample	Polymer	Mass/g	MM/g/mol
PLD165	F127	0.0498	12,600[†]
	P123	0.0464	5750[†]
PCL32	Z233[c]	0.0534	2600[‡]

[†] From Ref. [25].
[‡] From Ref. [27].

2.1. Cell culture

Penicillin–streptomycin antibiotic solution (P/S; 100 units/mL penicillin, 100 mg/mL streptomycin), Roswell Park Memorial Intitute-1640 (RPMI-1640), Dulbecco Modified Eagle Medium (DMEM), Leibovitz's/L^5 Medium (L-15), Phosphate-buffered saline 10x, pH 7.4 (PBS), fetal bovine serum (FBS) and 0.25 % (w/v) trypsin solution were purchased from Thermo-Fisher Scientific, USA. Human lung adenocarcinoma cells (A549) and cervical cancer cells (HeLa) were purchased from the American Type Culture Collection (ATCC), USA. Culture plates and dishes were obtained from Corning Inc. NY, USA.

All cell culture media and supplements were purchased from Gibco (Grand Island, NY, USA). A549 and HeLa cells were cultured in Dulbecco's Modified Eagle medium (DMEM). The medium was supplemented with 10 % fetal bovine serum, 2 mM L-glutamine and 100 U/mL Penicillin-Streptomycin. The cells were maintained at 37 °C in an incubator with a humidified atmosphere containing 5 % CO_2. In this study, 85 % cell confluence was utilised for experiments.

2.2. Cytotoxicity assay

A549 and HeLa cells were seeded at a density of 5×10^3 cells per well in 96-well plates for 24 hrs. Following the cells exposure to various concentrations of free and encapsulated DX (PLD165 and PCL32) ranging from 0 to 10 μg/mL for 24 and 48 hrs, cells viability was determined at indicated time points using the sulforhodamine (SRB) assay according to literature reports [30]. The optical density (OD) was measured by a Synergy H1 Multi-Mode Reader (BioTek Industries, Inc., VT, USA) at the wavelengths of 564 nm and of 690 nm, that was used as a reference. The cell viability (%) was calculated as

$$\frac{(OD_{564} - OD_{690})_{TREATED}}{(OD_{564} - OD_{690})_{UNTREATED}} \bullet 100$$

Each experiment was performed three times independently. The half maximal inhibitory concentration (IC_{50}) values were calculated using GraphPad Prism 8 (GraphPad Software, Inc., San Diego, CA).

2.3. Confocal Laser Scanning Microscopy (CLSM)

Cell uptake of DX loaded micelles (green fluorescence) was evaluated by using confocal laser scanning microscopy (CLSM). Briefly, A549 and HeLa cells were seeded in 96-well black plates with clear bottom at 5×10^3 cells density per well for 24 hrs. The cells were then incubated with free DX and encapsulated DX (PLD165 and PCL32) at concentrations of 1 and 5 μg/mL for 24 hrs. Subsequently, the cells were washed twice with phosphate buffered saline (PBS) and fixed with 4 % paraformaldehyde for 15 min at room temperature (RT). Cell nuclei were stained with the fluorescent dye Hoechst 33,342 (5 μg/mL) (Invitrogen, Waltham, MA, USA) for 15 min at RT. Images were acquired on a Zeiss LSM 880 confocal microscope (Carl Zeiss Microscopy, Jena, Germany).

3. Results and discussion

The literature value for the deprotonation constant of DX ammonium group (pK_{CN}) covers more than 1 pK unit. In any case, it is possible to

estimate that at the pH of 7.7 used in the preparation of the mixed micelles in the presence of NaC,[10,11] even considering the highest pK_{CN} (=9.25) reported in the literature [18], around 3 % of DX molecules are in the deprotonated form; this percentage rapidly increases when lower pK_{CN} values are used for its estimation at a fixed pH. By considering an average pK_{CN} value of 8.0, at any DX concentration at pH = 7.7 it is possible to estimate that 30 % of DX is in its deprotonated form. As mentioned before, the solubility properties of DX-NH_2 have been exploited in the literature for loading the drug in several delivery systems [12–15]. These systems proved to still retain the cell-killing capacity of DX because, once in the cells, at endosomal pH≈ 5 [31], the DX-NH_2 is readily protonated restoring the drug cationic form thus recovering the DX capability to act as DNA intercalating agent [2–4]. The slow kinetics of DX encapsulation in the proposed mixed micellar systems [10,11] appears therefore to be possibly ascribed to the low amount of the drug in the unprotonated form at pH 7.7. By increasing the pH the amount of the drug in the unprotonated form should clearly increase though it has to be kept in mind that DX stability largely decreases at increasing pH [32]. To verify whether this hypothesis was correct, a simple experiment was performed. DX solutions of the same concentration but at different pHs were prepared ([DX] = $2.20\bullet10^{-5}$ M; 50 mM TRIS•HCl buffer; 6.2 ≤ pH ≤ 8.5). 1.0 mL of each of these solutions was then layered over 0.5 mL of chloroform ($CHCl_3$; a solvent where DX can be safely considered insoluble). The two phases' systems were then vortex mixed for 30 s and then centrifuged (5 min; $1.3\bullet10^4$ r.p.m.). The two phases from all the tubes were then collected separately and both their fluorescence and absorption spectra acquired (Fig. 1 and Fig. A2). The utmost care was paid to limit to a minimum (<10 min) the exposure of DX to alkaline pHs to prevent any drug degradation.

The data showed that upon raising the pH the overall signal intensity in the water phase decreased thus indicating that a larger amount of DX was transformed into DX-NH_2 that was then extracted by the organic phase, as confirmed by the concomitant increase in the area of the fluorescence spectra relevant to the $CHCl_3$ phase (upper inset of Fig. 1, right hand axis, and Fig. A2). However, increasing the pH, one of the phenolic groups of the anthraquinone moiety of DX starts to get deprotonated; because both the monoanionic, $[DX\text{-}NH_2]^-$, and dianionic forms of DX, $[DX\text{-}NH_2]^=$, have distinct absorption spectra (Fig. A1) this effect can be monitored at 590 nm, a wavelength where neither DX nor DX-NH_2 show any appreciable absorption.[22] The ratio between the drug absorbances at 590 nm and at 483 nm (Fig. 1; upper inset – left hand axis) provides a mean to quickly evaluate the extent of this second deprotonation process (if any). At the pHs used in these experiments it could safely be assumed that the third deprotonation process did not contribute to the measured absorbance at 590 nm (Fig. A2) [17,22]. From the data reported in Fig. 1 it is evident that increasing the pH from slightly acidic (6.2) to mildly basic (8.5), an increasing amount of DX-NH_2 is formed and transferred to the organic phase but in parallel some $[DX\text{-}NH_2]^-$ forms as well. This results in a lower amount of DX-NH_2 extracted in $CHCl_3$ (Fig. 1 – upper inset) above pH≈ 8 because of the net negative charge appearing on the molecule. In choosing the right pH to test our hypothesis, i.e. that the rate limiting step in the DX internalization into the hydrophobic core of PM is the formation of the DX-NH_2 specie, a compromise has to be reached between the need to work at alkaline pH (to favour the DX-NH_2 formation) and the need to prevent the onset of the second deprotonation process that would decrease the amount of neutral DX-NH_2 and thus decrease the drug solubility in the apolar phase. From the data reported in Figs. 1 and A2, it appears evident that a pH value of 8.1 represents the right compromise. In passing, in a paper recently appeared in the literature, the deprotonation equilibrium $[DX-NH]_3^+/[DX-NH_2]$ has been exploited for the drug loading into silica-based nanocarriers [33], showing that also in that instance the maximum drug uptake was obtained working at mildly basic pHs.

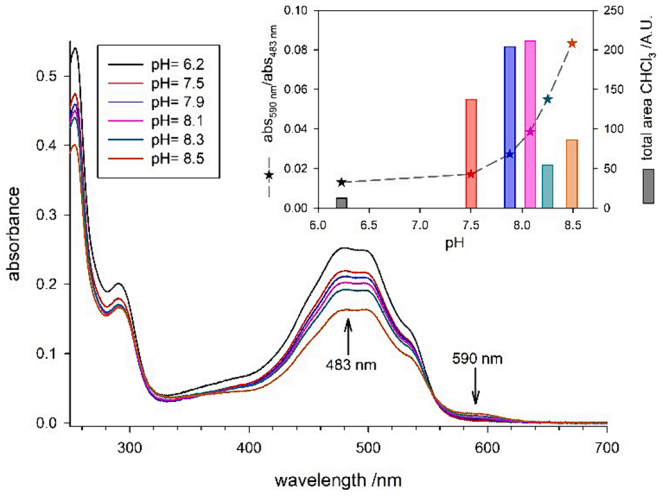

Fig. 1. Water phase DX absorption spectra (l = 1.0 cm) at different pHs (see legend) as obtained from the two phase experiments described in the text. The upper inset shows the ratio between the absorbances measured at 590 nm and those measured at 483 nm (left hand axis – same colours as in the main graph) together with the area of the fluorescence spectra of the $CHCl_3$ phase (right hand axis– same colours as in the main graph; the relevant fluorescence spectra are reported in Fig. A2 of the Appendix).

Therefore, we choose to evaluate the kinetics of incorporation of DX in the polymeric micellar phase at pH = 8.1. By considering the average pK_{CN} value of 8.0, this means that approximately 56 % of the drug molecules are in the unprotonated form at this working pH.

The PM systems investigated in this work were based or on a mixture of pluronics (F127/P123 in a molar ratio of 1:2, at pH = 8.1) or on the diblock copolymer MPEG-PCL. The choice to use also a PCL based copolymer whose performances to be compared with pluronics based PM was suggested by several papers showing the effectiveness of PCL based nanoparticles as drug delivery systems [34].

The incorporation of DX-NH_2 in the apolar core of the PM had three main consequences: (i) it led to a change in the relative intensity of the emission bands centred at around 560 nm (I_1) and 590 nm (I_2) [35], so that the ratio I_1/I_2 could be used to follow the kinetics of the drug incorporation in the different preparations; (ii) the exposure of the fluorophore to a less polar environment compared to water induced its fluorescence lifetime to increase, from 1.00 ns [36] to around 4 ns [10], therefore also the plot of $< \tau >$ vs. time could provide the same information on the internalization process; (iii) the almost doubling of DX fluorescence quantum yield (from around $3.9\bullet10^{-2}$ [36] to around $7.5\bullet10^{-2}$, this last value was calculated from the radiative DX lifetime of 53 ns [37] and the $\langle\tau\rangle$ of 4 ns measured in PM [10]).

In order to remove the non internalized drug, samples were dialyzed following a published procedure [10,11].

In the case of PM prepared with MPEG-PCL copolymer, the limiting values for I_1/I_2 (1.32) and for the $\langle\tau\rangle$ (3.22 ns) were slightly lower than those exhibited by the systems prepared with pluronics (Fig. 2 – insets). This is fully compatible with the less hydrophobic nature of the core of the MPEG-PCL micelles due to the presence of the ester functionality (Chart 1). Examples of fluorescence lifetime decay curves before and after dialysis are reported in the Appendix (Fig. A3); it is evident how the biexponential decays shown by the samples before the dialysis became single exponential after the dialysis indicating the removal of the fast decaying, not encapsulated drug (DX lifetime in water: 1.00 ns [36]).

As shown in Fig. 2 and as hypothesised, the incorporation kinetics at pH = 8.10 is much faster compared to that measured at the pH of the NaC solution: 5 days and 60 days [10], respectively, both the polymeric system investigated sharing the same uptake kinetics (Fig. 2 - insets). The relevant UV–Vis spectra together with the DLS time evolution for both systems are reported in Fig. A4. In order to compare the preparation procedure here proposed with that already published [10,11], i.e. to

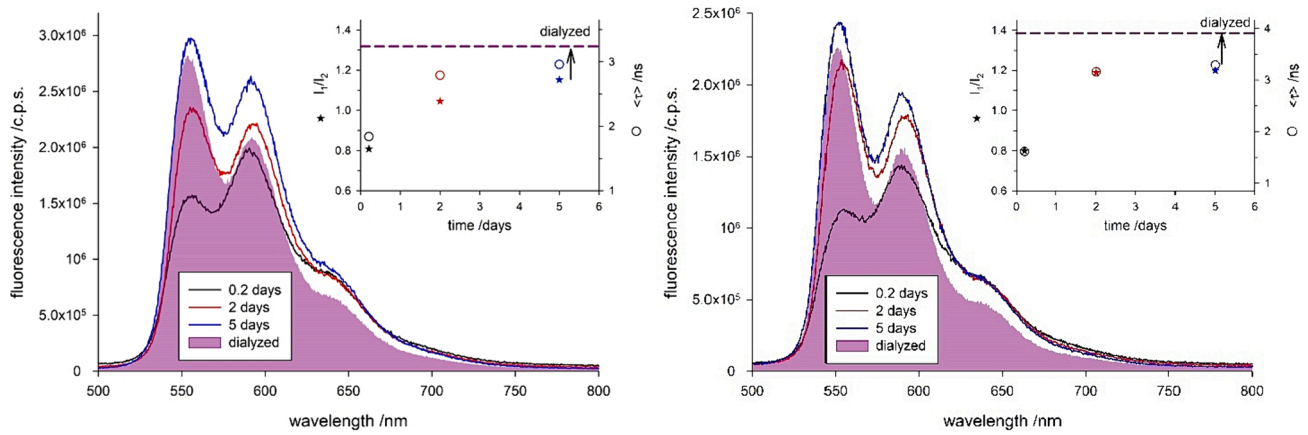

Fig. 2. Time evolution (see legends) of the fluorescence spectra of DX internalization in the presence of F127/P123 micelles (1 % w/V each polymer; right panel) and MPEG-PCL micelles (1 % w/V; left panel) prepared at pH = 8.10 and at a temperature of 45 °C. In both panels, the inset reports the time evolution of the I_1/I_2 ratio (left hand axis – star symbols) and of the average fluorescence lifetime ($\langle\tau\rangle$) measured at 560 nm (right hand axis – hollow circles) for both samples. The shaded spectra refer to the dialyzed samples and the dashed horizontal lines in both insets are the limiting value reached for the different quantities in the plots after the dialysis. For steady state fluorescence, λ_{exc} = 410 nm; slits 1.5/1.5 nm. For TCSPC measurements, λ_{exc} = 378 nm; 20 MHz repetition rate; 33 ps time resolution. In both cases, 0.3x0.3 cm quartz cuvette; T = 45 °C.

determine the role played by NaC and pH in the preparation of the pluronics based polymeric micelles, different samples were also prepared in the presence of NaC (see the relevant section in the Appendix – Fig. A5).

At the end of the preparation, after the dialysis, the polymeric micelles were freeze-dried and stored at −25 °C under Ar. This procedure was performed for several reasons. First of all, the drug stability increases when in solid state; therefore, the shelf life of freeze-dried samples greatly increases. Then, freeze-dried samples are more conveniently exchangeable among partner laboratories (as done in this work for the evaluation of the therapeutic potential of our formulations), a procedure that often requires their expedition via couriers. Last, but not least, while drug loaded PMs in solution are stable only if their temperature is above the CMT of the polymers, the freeze-dried samples are stable even at room temperature or in the freezer for several weeks. To evaluate whether the freeze-drying procedure altered both their dimensions and size distribution and/or induced any drug leaking/degradation, samples (from a different batch respect to those already shown) have been re-suspended in warm (45 °C and 37 °C) bidistilled water and characterized again for drug leaking (by fluorescence and UV–Vis spectroscopies) and dimensional changes, if any (by DLS). The results of these tests are collected in the relevant section in the Appendix (Figs. A6 and A7). PM incorporating the drug prepared with both pluronics and MPEG-PCL were also tested to evaluate the effect of repeated freeze–thaw cycles (Fig. A8).

The evaluation of the drug loading in the PMs, expressed as mole percent (DL_M) and weight percent (M_L) was obtained following the experimental procedure described in detail in the relevant section of the Appendix (Figs. A9 and A10; Tables A1 and A2). Briefly, to determine the amount of drug present in the inner, hydrophobic, compartment of the micelles, the absorption spectra relevant to the dialyzed samples have been used (Fig. A4), by exploiting the molar extinction coefficient of the drug calculated in *n*-hexane [26]. Since the calculated and experimental doxorubicin spectra cross at three wavelengths, namely 510.0 ± 0.5, 524.5 ± 0.5 and 533.0 ± 0.5 nm (Fig. A9), the absorbance values shown by the drug at these wavelengths can be used as a control to calculate, from the experimental absorption spectra of the just prepared samples (Fig. A4 – 0.2 days traces), the total concentration of DX in the just prepared samples ($[DX]_{starting}$ – Table A1). This is possible because the molar extinction coefficient at these wavelengths will account for both DX in the bulk and in the interior of the micelles, while that at 541 nm allows to determine only the concentration of the drug secluded in the hydrophobic core of the polymeric micelles (ϵ_{541} = 7319 M^{-1} cm^{-1}; from ref. [26]) by using the absorbance shown by the dialyzed samples at the wavelength of 541 nm ($[DX]_{dialyzed}$). The average values obtained for the $[DX]_{starting}$ in both systems (last line of Table A1) are in excellent agreement with the starting $[DX]_{anal}$ (see Materials and Methods section). Once DL_M and M_L were determined (Table A2), these quantities allowed to test our PMs for their therapeutic potential, according to the experiments reported hereafter.

DX loaded PM were administered to two different cancer cells lines, HeLa and A549, and the delivering evaluated by Confocal Laser Scanning Microscopy (CLSM - Fig. 3). Cells were as well exposed to free DX as control. Cell nuclei were stained with Hoechst 33342. The superimposed transmission and fluorescence images taken after one day of exposure of HeLa cells PM are shown in Fig. A11. In the case of the control experiment, cells fluorescence could be detected just in the nuclei; Hoechst 33,342 (blue) and DX (green) fully overlap, clearly indicating that within 24 hrs all the DX already reached the nuclei. For the two DX loaded micellar systems (PCL32 and PLD165) within the same time interval, the DX fluorescence was mainly detected outside the nuclei, where the Hoechst 33342 fluorescence was still clearly appreciable. Spots of DX fluorescence could be appreciated in the nucleus of some cells. This means that some of the DX was being slowly released from the micelles. The confocal images revealed the same trend for both cell lines: free DX was in the nuclei, while the encapsulated drug was mainly present in the cytoplasm.

The slow release of the encapsulated drug inside the cells should have consequences on its cytotoxicity since it must reach the nucleus to induce cell death.

To validate this result, a cytotoxicity test was conducted.

The assessment of cell viability was performed by a sulforhodamine B (SRB) assay, which can determine cell density based on the measurement of cellular protein content. The half-maximal (50 %) inhibitory concentration (IC_{50}) data for free DX, encapsulated DX, and MPEG-PCL diblock copolymer micelles without DX (Z233) are shown in Table 2. Pluronics cytotoxicity was not investigated since it has been already assessed as non-toxic for the cells in the range of concentrations used throughout this work [11].

The effect of free and encapsulated drug on cell viability were evaluated in two cancer cell lines, HeLa and A549 cells, at two different timepoints (24 and 48 hrs) with concentrations of DX from 0 to 10 μg/mL (0–17 μM). A control experiment was performed with free DX at the same concentration as in the PM.

As shown in Fig. 4, free DX dramatically reduced cell viability in both cell lines in a dose- and time-dependent manner compared to

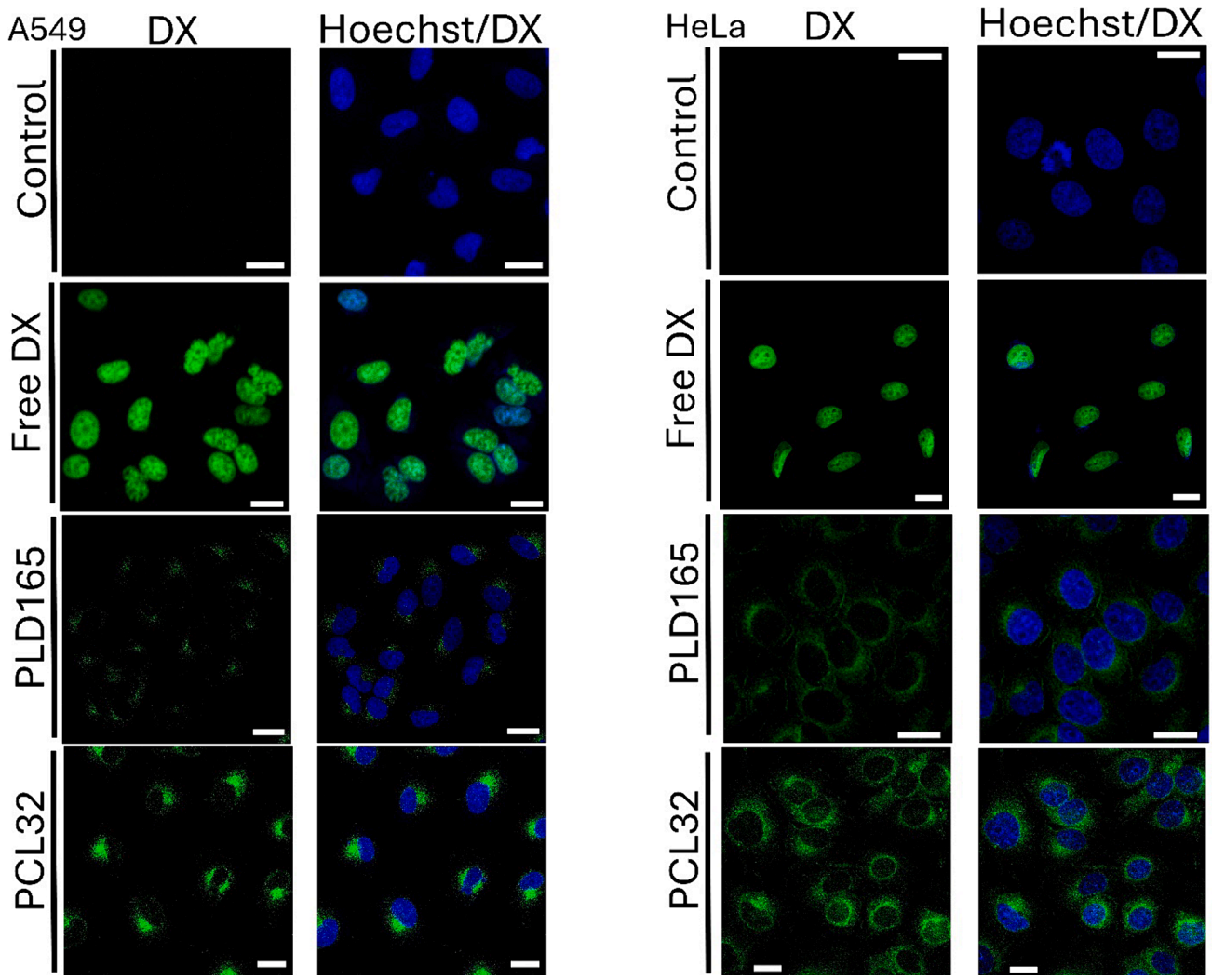

Fig. 3. Confocal Laser Scanning Microscopy (CLSM) images of two cell lines (HeLa and A549; see legend) after 24 hrs from the exposure to the same amount of drug (5 μg/mL) as free (Free-DX) or encapsulated in PM (PLD 165 and PCL 32) drug. Nuclei were stained with Hoechst 33342 dye (blue fluorescence) while the green fluorescence is to be referred to DX; bar lengths adjusted to 20 μm. (For interpretation of the references to colour in this figure legend, the reader is referred to the web version of this article.)

Table 2
Cell viability (IC_{50}; μg/mL) for the encapsulated (PLD165 and PCL 32) and free DX and for the MPEG-PCL diblock copolymer (Z233) as determined by the sulforhodamine B assay.

		IC_{50} (μg/mL)			
		DX	PLD165	Z233	PCL32
HeLa	24 hrs	0.29	>10	>10	>10
	48 hrs	0.04	>10	>10	2.74
A549	24 hrs	1.92	>10	>10	7.86
	48 hrs	0.12	5.64	>10	3.25

encapsulated DX. Free DX showed a IC_{50} of 0.29 and 1.62 μg/mL at 24 hrs for HeLa and A549, respectively, that decreased to 0.04 μg/mL (HeLa) and to 0.12 μg/mL (A549) at 48 hrs (Table 2). For the encapsulated drug, at 24 hrs, we observed that the IC_{50} for all formulations was higher than 10 μg/mL for both cancer cell lines, with only the IC_{50} of PCL32 for A549 being lower than 10 μg/mL (7.86 μg/mL). At 48 hrs, the IC_{50} of PCL32 was 2.74 μg/mL, whereas the IC_{50} for other formulations was higher than 10 μg/mL. In A549 cells, the IC_{50} for PLD165 and PCL32 were 5.64 μg/mL and 3.25 μg/mL, respectively (Table 2). Additionally, the IC_{50} for the MPEG-PCL diblock copolymer (Z233) was consistently higher than 10 μg/mL for both cell lines and both incubation times. The most cytotoxic formulations of PM loaded with DX at 48 hrs required more than 30 times the amount of free DX to induce 50 % cell death. It is clear from these experiments that the availability of DX in the nucleus is lower when the DX is encapsulated.

Cytotoxicity test confirmed the conclusion drawn from the confocal images (Fig. 3), which showed that despite the high uptake of DX in the cells, it was mostly confined to the cytoplasm. Such results hint that DX remains encapsulated in the micelles even if these are incorporated by the cells in the endosomes otherwise the drug would have reached the nuclei much faster. Taking this observation onto account, it is reasonable to presume that the slow release process is a consequence of the protonation of DX-NH_2 at the endosomal pH. Such a process should involve just those drug molecules located at the interface separating the apolar core and the hydrophilic shell of the PM; only this fraction of DX-NH_2 molecules would be capable, once protonated, to diffuse from the micelles to the nuclei. Most probably, a concentration gradient is created from the inner core to the periphery of the micelles, which triggers a release that is rather slow, as evidenced by both SRB and confocal microscopy.

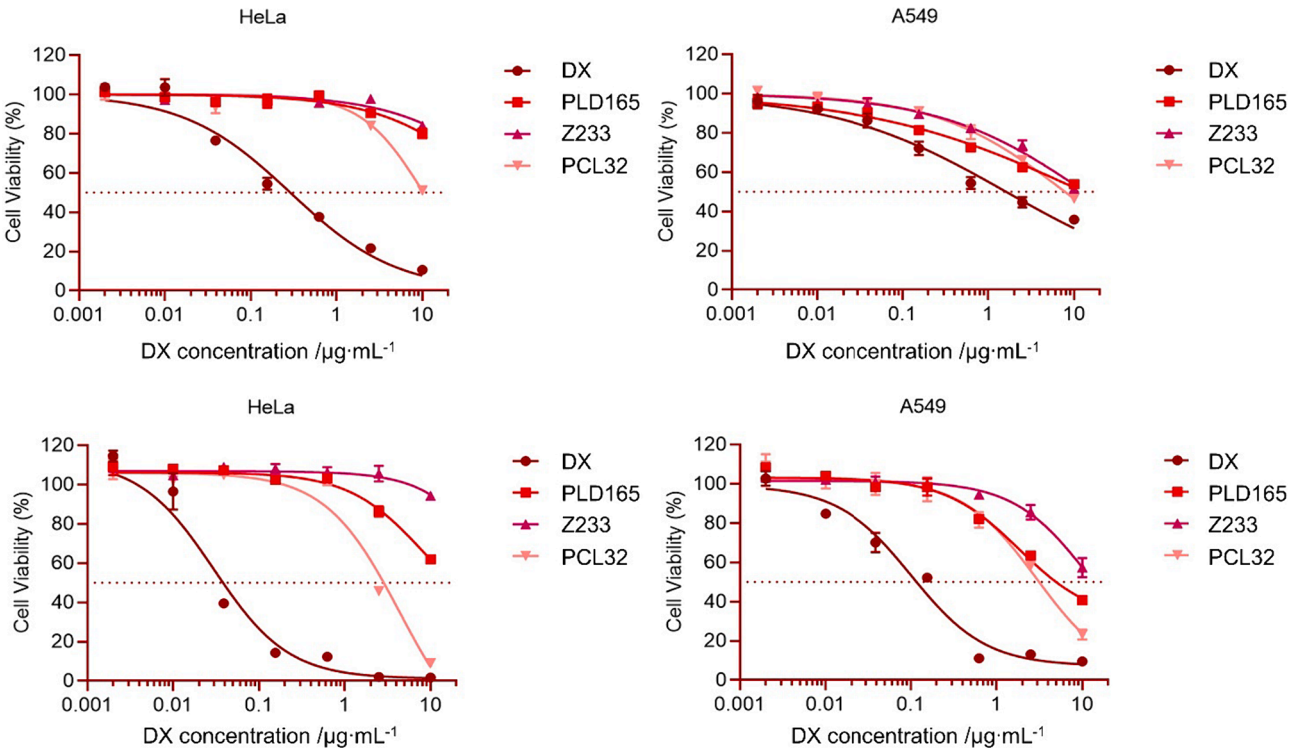

Fig. 4. Cell viability as a function of DX concentration for HeLa and A549 cell lines after 24 hrs (upper panels) and 48 hrs (lower panels) of incubation with increasing amount of free DX, encapsulated DX (PLD165 and PCL 32) and for the MPEG-PCL diblock copolymer alone (Z233). Error bars represent the standard deviation (n = 3); when not visible, they are well within the symbols.

4. Conclusions

In synthesis, our results show that pH controls the encapsulation of DX into the hydrophobic core of pluronics and MPEG-PCL micelles in terms of both quantity and rate. An optimal pH of 8.1 has been found. At this pH deprotonation of the ammonium group of DX takes place effectively while the phenolic groups of the anthraquinone moiety remain uncharged. At higher pHs the phenolic groups acquire a negative charge that prevents translocation of DX into the organic phase. By tracing the time evolution of the I_1/I_2 emission bands of DX as well as the its fluorescence lifetime, a 5 days kinetics of incorporation of the drug in the micelles was observed, much faster than the 60 days required for its encapsulation in the presence of NaC [10,11]. As in detail described in the Appendix, not only the DX incorporation kinetics is much faster in the experimental conditions assessed in this work but also the incorporation yield (expressed both as mole percent – DL_M – and weight percent – ML; see Table A1) is appreciably higher: 56 % against 27 % previously obtained [11] and even higher in the case of the MPEG-PCL based polymeric micelles (62 %). The data here presented provide information also on the PM stability in terms of dimensions and drug leakage after freeze-drying and repeated freeze and thaw cycles, with the polymeric micelles prepared with MPEG-PCL showing the best performances (see Figs. A5, A6 and A7 in the Appendix). Our results provide insight on the sensitivity of DX to pH for moving into an organic phase. We establish for the first time here the optimal pH for the encapsulation of DX in organic cores, pH = 8.1, which is highly relevant for pharmaceutical formulations of the drug. Moreover, the proposed method of preparation of PM incorporating the DX represents a greener alternative to those methods proposed in the literature making use of organic bases to deprotonate DX then extracting the formed DX-NH_2 with chlorinated solvents. Further work will focus in the future on tracing the release of DX intracellularly by fluorescence lifetime imaging (FLIM), also extending this method of PM preparation to other anthracyclines and/or polymers with the aim of also increasing the amount of internalized drug since, as other PM proposed in the literature over the years, the drug loading is still far from those shown by liposomial formulations already on the market.

CRediT authorship contribution statement

Lucrezia Desiderio: Investigation, Data curation, Methodology. **Natalie Solfried Gjerde:** Investigation, Data curation, Methodology. **Elisamaria Tasca:** Investigation, Data curation, Methodology. **Luciano Galantini:** Methodology. **Irantzu Llarena:** Investigation. **Paolo Di Gianvincenzo:** Investigation. **Sunisa Thongsom:** Investigation. **Sergio E. Moya:** Funding acquisition, Conceptualization, Supervision, Writing – review & editing. **Mauro Giustini:** Funding acquisition, Conceptualization, Supervision, Validation, Writing – review & editing.

Declaration of competing interest

The authors declare that they have no known competing financial interests or personal relationships that could have appeared to influence the work reported in this paper.

Data availability

Data will be made available on request.

Acknowledgements

The Authors wish to acknowledge Prof. Bo Nyström for the kind gift of the MPEG-PCL copolymer and Prof. A.M. Giuliani for critical reading of the manuscript.

The financial support of “La Sapienza” (Ateneo 2021) is kindly acknowledged.

MG wishes to thank C.S.G.I. for partial financial support and Dr. Friedrich Menges for permitting the use of his software Spectragryph

(Ver. 1.2.16).

S.E.M. acknowledges the financial support of ID2020-114356RB-I00 project from the Ministry of Science and Innovation of the Government of Spain. This work was performed under the Maria de Maeztu Units of Excellence Program from the Spanish State Research Agency - Grant no. MDM-2017-0720.

Finally, the Authors wish to thank the Reviewers for their observations and precious suggestions.

Appendix A. Supplementary material

Supplementary data to this article can be found online at https://doi.org/10.1016/j.jcis.2024.03.101.

References

[1] O. Tacar, P. Sriamornsak, C.R. Dass, Doxorubicin: an update on anticancer molecular action, toxicity and novel drug delivery systems, J. Pharm. Pharmacol. 65 (2012) 157–170, https://doi.org/10.1111/j.2042-7158.2012.01567.x.

[2] C. Pérez-Arnaiz, N. Busto, J.M. Leal, B. García, New insights into the mechanism of the DNA/doxorubicin interaction, J. Phys. Chem. b. 118 (2014) 1288–1295, https://doi.org/10.1021/jp411429g.

[3] O. Tacar, P. Sriamornsak, C.R. Dass, Doxorubicin: An update on anticancer molecular action, toxicity and novel drug delivery systems, J. Pharm. Pharmacol. 65 (2013) 157–170, https://doi.org/10.1111/j.2042-7158.2012.01567.x.

[4] J.B. Chaires, A thermodynamic signature for drug – DNA binding mode, Arch. Biochem. Biophys. 453 (2006) 26–31, https://doi.org/10.1016/j.abb.2006.03.027.

[5] S.A. Abraham, D.N. Waterhouse, L.D. Mayer, P.R. Cullis, T.D. Madden, M.B. Bally, The liposomal formulation of doxorubicin, Methods Enzymol. 391 (2005) 71–97, https://doi.org/10.1016/S0076-6879(05)91004-5.

[6] K. Mross, B. Niemann, U. Massing, C.E. Swenson, Pharmacokinetics of liposomal doxorubicin (TLC-D99; Myocet) in patients with solid tumors: an open-label, single-dose study, Cancer Chemother. Pharmacol. 54 (2004) 514–524, https://doi.org/10.1007/s00280-004-0825-y.

[7] Y. Barenholz, Doxil®–the first FDA-approved nano-drug: lessons learned, J. Control. Release. 160 (2012) 117–134, https://doi.org/10.1016/j.jconrel.2012.03.020.

[8] S. Rivankar, An overview of doxorubicin formulations in cancer therapy, J. Cancer Res. Ther. 10 (2014) 853, https://doi.org/10.4103/0973-1482.139267.

[9] E. Blanco, H. Shen, M. Ferrari, Principles of nanoparticle design for overcoming biological barriers to drug delivery, Nat. Biotechnol. 33 (2015) 941–951, https://doi.org/10.1038/nbt.3330.

[10] E. Tasca, A. Del Giudice, L. Galantini, K. Schillén, A.M. Giuliani, M. Giustini, A fluorescence study of the loading and time stability of doxorubicin in sodium cholate/PEO-PPO-PEO triblock copolymer mixed micelles, J. Colloid Interface Sci. 540 (2019) 593–601, https://doi.org/10.1016/j.jcis.2019.01.075.

[11] E. Tasca, P. Andreozzi, A. Del Giudice, L. Galantini, K. Schillén, A.M. Giuliani, M.D. L. Angeles, S.E. Moya, M. Giustini, Poloxamer/sodium cholate co-formulation for micellar encapsulation of doxorubicin with high efficiency for intracellular delivery: an in-vitro bioavailability study, J. Colloid Interface Sci. 579 (2020) 551–561, https://doi.org/10.1016/j.jcis.2020.06.096.

[12] E.R. Gillies, J.M.J. Fréchet, J.M.J. Fre, pH-responsive copolymer assemblies for controlled release of doxorubicin, Bioconjug. Chem. 16 (2005) 361–368, https://doi.org/10.1021/bc049851c.

[13] D. Missirlis, R. Kawamura, N. Tirelli, J.A. Hubbell, Doxorubicin encapsulation and diffusional release from stable, polymeric, hydrogel nanoparticles, Eur. J. Pharm. Sci. 29 (2006) 120–129, https://doi.org/10.1016/j.ejps.2006.06.003.

[14] X. Jin, B. Zhou, L. Xue, W. San, Soluplus® micelles as a potential drug delivery system for reversal of resistant tumor, Biomed. Pharmacother. 69 (2015) 388–395, https://doi.org/10.1016/j.biopha.2014.12.028.

[15] A. Mahdieh, H. Motasadizadeh, H. Yeganeh, B. Nyström, R. Dinarvand, Redox-responsive waterborne polyurethane nanocarriers for targeted doxorubicin delivery, Int. J. Pharm. 628 (2022) 122275, https://doi.org/10.1016/j.ijpharm.2022.122275.

[16] R. Kiraly, R.B. Martin, Metal ion binding to daunorubicin and quinizarin, Inorg. Chim. Acta. 67 (1982) 13–18, https://doi.org/10.1016/S0020-1693(00)85033-1.

[17] H. Beraldo, A. Garnier-Suillerot, L. Tosi, Copper(II)-adriamycin complexes. A circular dichroism and resonance raman study, Inorg. Chem. 22 (1983) 4117–4124, https://doi.org/10.1021/ic00168a058.

[18] T. Yotsuyanagi, N. Ohata, N. Tanaka, K. Ikeda, Complex formation between Gallium(III) and adriamycin in aqueous solutions, Chem. Pharm. Bull. 38 (1990) 3102–3106.

[19] L. Messori, C. Temperini, F. Piccioli, F. Animati, C. Di Bugno, P. Orioli, Solution chemistry and DNA binding properties of MEN 10755, a novel disaccharide analogue of doxorubicin, Bioorg. Med. Chem. 9 (2001) 1815–1825, https://doi.org/10.1016/S0968-0896(01)00092-X.

[20] R.J. Sturgeon, S.G. Schulman, Electronic absorption spectra and protolytic equilibria of doxorubicin: direct spectrophotometric determination of microconstants, J. Pharm. Sci. 66 (1977) 958–961, https://doi.org/10.1002/jps.2600660714.

[21] Z. Fülöp, R. Gref, T. Loftsson, A permeation method for detection of self-aggregation of doxorubicin in aqueous environment, Int. J. Pharm. 454 (2013) 559–561, https://doi.org/10.1016/j.ijpharm.2013.06.058.

[22] G. Razzano, V. Rizzo, A. Vigevani, Determination of phenolic ionization constants of anthracyclines with modified sustitution pattern of anthraquinone chromophore, Farm. 45 (1990) 215–222.

[23] E. Tasca, J. Alba, L. Galantini, M. D'Abramo, A.M. Giuliani, A. Amadei, G. Palazzo, M. Giustini, The self-association equilibria of doxorubicin at high concentration and ionic strength characterized by fluorescence spectroscopy and molecular dynamics simulations, Colloids Surf. A Physicochem. Eng. Asp. 577 (2019) 517–522, https://doi.org/10.1016/j.colsurfa.2019.06.005.

[24] A. Vigevani, M.J. Williamson, Doxorubicin, in: Anal. Profiles Drug Subst. Excipients, 1981, pp. 245–274. doi:10.1016/S0099-5428(08)60143-4.

[25] P. Singla, S. Garg, J. McClements, O. Jamieson, M. Peeters, R.K. Mahajan, Advances in the therapeutic delivery and applications of functionalized Pluronics: a critical review, Adv. Colloid Interface Sci. 299 (2022) 102563, https://doi.org/10.1016/j.cis.2021.102563.

[26] C.G. Chen, A.N. Nardi, M. Giustini, M. D'Abramo, Absorption behavior of doxorubicin hydrochloride in visible region in different environments: a combined experimental and computational study, Phys. Chem. Chem. Phys. 24 (2022) 12027–12035, https://doi.org/10.1039/d1cp05182b.

[27] N.S. Gjerde, A. Del Giudice, K. Zhu, K.D. Knudsen, L. Galantini, K. Schillén, B. Nyström, Synthesis and characterization of a thermoresponsive copolymer with an LCST–UCST-like behavior and exhibiting crystallization, ACS Omega. 8 (2023) 31145–31154, https://doi.org/10.1021/acsomega.3c03162.

[28] B. Porsch, R. Laga, J. Horský, C. Koňák, K. Ulbrich, Molecular weight and polydispersity of calf-thymus DNA: static light-scattering and size-exclusion chromatography with dual detection, Biomacromolecules. 10 (2009) 3148–3150, https://doi.org/10.1021/bm900768j.

[29] M.S. Ibrahim, Voltammetric studies of the interaction of nogalamycin antitumor drug with DNA, Anal. Chim. Acta. 443 (2001) 63–72, https://doi.org/10.1016/S0003-2670(0)01184-9.

[30] S. Thongsom, W. Suginta, K.J. Lee, H. Choe, C. Talabnin, Piperlongumine induces G2/M phase arrest and apoptosis in cholangiocarcinoma cells through the ROS-JNK-ERK signaling pathway, Apoptosis. 22 (2017) 1473–1484, https://doi.org/10.1007/s10495-017-1422-y.

[31] Y.-B. Hu, E.B. Dammer, R.-J. Ren, G. Wang, The endosomal-lysosomal system: from acidification and cargo sorting to neurodegeneration, Transl. Neurodegener. 4 (2015) 18, https://doi.org/10.1186/s40035-015-0041-1.

[32] M.J.H. Janssen, D.J.A. Crommelin, G. Storm, A. Hulshoff, Doxorubicin decomposition on storage. Effect of pH, type of buffer and liposome encapsulation, Int. J. Pharm. 23 (1985) 1–11, https://doi.org/10.1016/0378-5173(85)90217-0.

[33] A. Adam, S. Harlepp, F. Ghilini, G. Cotin, B. Freis, J. Goetz, S. Bégin, M. Tasso, D. Mertz, Core-shell iron oxide@stellate mesoporous silica for combined near-infrared photothermia and drug delivery: influence of pH and surface chemistry, Colloids Surfaces A Physicochem. Eng. Asp. 640 (2022) 128407, https://doi.org/10.1016/j.colsurfa.2022.128407.

[34] V. Taresco, I. Tulini, I. Francolini, A. Piozzi, Polyglycerol adipate-grafted polycaprolactone nanoparticles as carriers for the antimicrobial compound usnic acid, Int. J. Mol. Sci. 23 (2022) 14339, https://doi.org/10.3390/ijms232214339.

[35] K.K. Karukstis, E.H.Z. Thompson, J.A. Whiles, R.J. Rosenfeld, Deciphering the fluorescence signature of daunomycin and doxorubicin, Biophys. Chem. 73 (1998) 249–263, https://doi.org/10.1016/S0301-4622(98)00150-1.

[36] P. Changenet-barret, T. Gustavsson, D. Markovitsi, I. Manet, S. Monti, Unravelling molecular mechanisms in the fluorescence spectra of doxorubicin in aqueous solution by femtosecond fluorescence spectroscopy, Phys. Chem. Chem. Phys. 15 (2013) 2937–2944, https://doi.org/10.1039/c2cp44056c.

[37] E. Tasca, M. D'Abramo, L. Galantini, A.M. Giuliani, N.V. Pavel, G. Palazzo, M. Giustini, A stereochemically driven supramolecular polymerisation, Chem. - A Eur. J. 24 (2018) 8195–8204, https://doi.org/10.1002/chem.201800644.